

Generation of high-flux attosecond extreme ultraviolet continuum with a 10 TW laser

Y. Wu, E. Cunningham, H. Zang, J. Li, M. Chini et al.

Citation: *Appl. Phys. Lett.* **102**, 201104 (2013); doi: 10.1063/1.4807395

View online: <http://dx.doi.org/10.1063/1.4807395>

View Table of Contents: <http://apl.aip.org/resource/1/APPLAB/v102/i20>

Published by the [American Institute of Physics](http://www.aip.org).

Additional information on *Appl. Phys. Lett.*

Journal Homepage: <http://apl.aip.org/>

Journal Information: http://apl.aip.org/about/about_the_journal

Top downloads: http://apl.aip.org/features/most_downloaded

Information for Authors: <http://apl.aip.org/authors>

ADVERTISEMENT

minus k[®] TECHNOLOGY *20 years* **Improve your Images with Minus K's**
Negative-Stiffness Vibration Isolation

Workstations & Optical Tables **Bench Top Isolators** **Without Minus K** **With Minus K** **Floor Platforms**

Custom Applications **Multi Isolator Systems**

The advertisement features several images: two optical tables, two bench top isolators, three multi-isolator systems, and two floor platforms. It also includes two side-by-side topography images labeled 'Without Minus K' and 'With Minus K', both showing a 'Topography - Scan forward' view with a color scale from 0µm to 25µm. The 'Without Minus K' image shows a highly textured surface, while the 'With Minus K' image shows a much smoother surface. Logos for NASA, ESA, JPL, and JWST are displayed at the bottom left.

Generation of high-flux attosecond extreme ultraviolet continuum with a 10 TW laser

Y. Wu,¹ E. Cunningham,¹ H. Zang,^{1,2} J. Li,¹ M. Chini,¹ X. Wang,^{1,3} Y. Wang,¹ K. Zhao,¹ and Z. Chang^{1,a)}

¹CREOL and Department of Physics, University of Central Florida, Orlando, Florida 32816, USA

²Institute of Atomic and Molecular Physics, Sichuan University, Chengdu 610054, China

³Department of Physics, National University of Defense Technology, Hunan 410073, China

(Received 19 March 2013; accepted 4 May 2013; published online 21 May 2013)

We report a laser system that delivers 15 fs pulses with 200 mJ energy at a 10 Hz repetition rate. The broadband spectrum extending from 700 nm to 900 nm was obtained by seeding a two-stage Ti:sapphire chirped-pulse power amplifier with sub-mJ white-light pulses from a gas-filled hollow-core fiber. With this laser, an extreme ultraviolet (XUV) super-continuum supporting 230 as isolated attosecond pulses at 35 eV was generated using the generalized double optical gating technique. The XUV pulse energy was ~ 100 nJ at the exit of the argon gas target.

© 2013 AIP Publishing LLC. [<http://dx.doi.org/10.1063/1.4807395>]

Time-resolved experiments with attosecond resolution have been performed thus far by combining weak extreme ultraviolet (XUV) attosecond pulses with stronger near infrared (NIR) femtosecond lasers, which has limited the scope of attosecond science to the study of laser-induced strong-field processes. Isolated attosecond pulses with high photon flux are required for conducting true attosecond pump–attosecond probe experiments to study electron dynamics in atoms, molecules, and condensed matter.¹ At current, significant progress has been made in developing “gating” schemes capable of isolating a single attosecond pulse from high harmonic generation (HHG),² but these XUV pulses are still restricted to energies less than 10 nJ.³ This is because most generation schemes require few-cycle driving NIR pulses that are similarly limited in their energies to ~ 1 mJ.

In order to scale the isolated attosecond pulse energy to the microjoule level, driving lasers with higher power are required. While the option of using optical parametric chirped pulse amplification (OPCPA) offers the advantage of few-cycle laser pulses with scalable energy, the specialized pump laser technology for OPCPA is still underdeveloped. On the other hand, widely available Ti:Sapphire-based chirped-pulse amplification (CPA) laser systems are capable of achieving ~ 100 TW peak power, but their output pulses—typically lasting 30 fs or longer—contain too many optical cycles to be used with even the least-restrictive gating schemes.

In this letter, we report the generation of 100 nJ isolated attosecond pulses from a unique high-energy, short-pulse laser system employing Generalized Double Optical Gating (GDOG), which is a combination of polarization gating and two-color gating.⁴ In GDOG, the laser field is manipulated to be linearly polarized only within a single-optical-cycle “gate” at the center of the pulse, whereas the leading and trailing edges are elliptically polarized. A linearly polarized second-harmonic field is added to break the field symmetry, restricting attosecond pulse generation to a single event

within the gate. While the GDOG method can be applied to both few and multi-cycle lasers, the driving laser pulse duration remains a key parameter, as only the energy contained in the linearly polarized cycle of the laser contributes to the generation of the isolated attosecond pulse. If the pulse duration is too long, the leading cycles of the pulse pre-ionize many of the available atoms before the arrival of the linear gated cycle, thus reducing the conversion efficiency. This effect can be mitigated by keeping the duration of the driving laser pulse as short as possible. To this end, we developed a Ti:sapphire laser system optimized to provide both high-energy (200 mJ) and short-duration (15 fs) pulses for implementing GDOG.

The optical layout of the driving laser and the setup for generating isolated attosecond pulses is shown schematically in Fig. 1. The main challenge of reaching 15 fs above the 10 TW level is the suppression of spectral gain narrowing. This was resolved by distributing the high gain of the system ($\sim 10^9$) over two chirped-pulse amplifiers. The significant spectral narrowing in the first CPA, which has a total gain of 10^6 , is recovered by spectral broadening in a neon gas-filled hollow-core fiber. The resulting millijoule-level white-light pulses are then used to seed the second CPA. Even though the pulses proceed to reach energies of several hundred millijoule, the final spectrum is spared from severe gain narrowing because the pulses only experience a total gain of 10^3 —orders of magnitude smaller than what is typical of other 10 TW-class lasers.

Spectra from various stages of the laser are shown in Fig. 2. The first CPA consists of a two-stage multi-pass Ti:sapphire amplifier seeded by a broadband Ti:sapphire oscillator. The output pulses (1 kHz, 20 fs, 1.5 mJ) are launched into a neon-filled hollow-core fiber (1.5 m length, 450 μm core diameter, 1.4 bar gas pressure) to generate a white-light continuum with spectrum from 550 nm to 950 nm. The center mode of the spectrally broadened pulses is used to seed the second CPA.⁵

The sub-mJ broadband seed pulses first pass through an Offner-type stretcher,⁶ whose mirror curvatures are

^{a)}Zenghu.Chang@ucf.edu

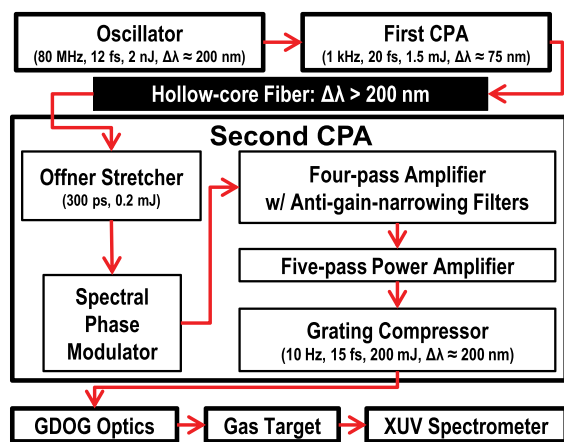


FIG. 1. Block diagram representing the 10 Hz, 10 TW, Ti:sapphire-based laser system with accompanying HHG and measurement setup.

optimized from 680 nm to 900 nm to minimize spatial chirp. The 300 ps, 0.2 mJ positively chirped pulses are then amplified to 30 mJ in a four-pass amplifier operating at 10 Hz. This Brewster-cut Ti:sapphire crystal is pumped from both sides by relay-imaged portions of a Q-switched frequency-doubled Nd:YAG laser (Quanta Ray Pro 350). Specially designed filters with a transmission minimum near 780 nm are inserted into the first three passes to alleviate gain-narrowing effects in this stage.⁷

The second stage power amplifier employs a large-area, flat-cut Ti:sapphire crystal, which is pumped on one side by the remainder of the first-stage pump laser and on the other side by the full energy of another Nd:YAG laser (Quanta Ray Pro 350) with high M^2 factor. Two diffractive optical

homogenizers regulate the profiles of the pump beams, ensuring that no “hot” structures are generated in the NIR pulse during amplification.⁸ Both stages are water-cooled to room temperature, while divergent lenses are used to compensate the thermal lens. The energy of the amplified pulse reaches up to 700 mJ. The spectrum of these pulses extends from 700 nm to 900 nm, which supports 12.2 fs transform-limited pulses. The long term stability, RMS/mean, is 1.6%, whereas the shot-to-shot fluctuation is $\pm 4.4\%$ for 99% of all laser pulses over 6 h.

The beam is expanded to a diameter of 35 mm before it is sent under vacuum to a pulse compressor, which features a pair of 1400 l/mm gratings and an overall throughput of 50%. The pulse compression was characterized by a single-shot second-harmonic FROG. First, the separation and incident angle of the gratings were fine-tuned manually to obtain a spectral phase that changed only gradually over any narrow range. This was done so that the high-order phase distortions could be compensated by a low-loss, 4 f -zero-dispersion adaptive phase modulator,⁹ which is located between the stretcher and the first amplification stage. In the phase modulator, the laser beam is angularly dispersed by a Brewster-cut SF10 prism and re-collimated onto 50 mm-long, 20-channel linear piezoelectric deformable mirror (OKO Technologies) using a dielectric mirror with a focal length of 1.5 m. The overall transmission of this phase modulator reaches 85% for a bandwidth over 200 nm.

For optimizing the pulse compression, the FROG traces were used as the fitness function for an evolutionary algorithm, which controlled the voltages applied to the deformable mirror actuators. After running the algorithm to convergence (usually ~ 20 iterations), a pulse duration of 15.1 fs could be obtained, as displayed in Fig. 3. The energy of the pulse was 200 mJ for a 400 mJ input, which indicates that the peak power of the laser reached 13 TW. Even higher power (30 TW) is expected once the current gratings are replaced with a larger-dimension, higher-throughput pair capable of accommodating the 700 mJ input. The carrier-envelope phase (CEP) of the laser is not stabilized due to two major challenges for CEP locking. First, the maximum speed of f -to- $2f$ CEP measurement is limited to the laser repetition rate, which makes it difficult to compensate phase variations faster than 10 Hz. Second, the large shot-to-shot fluctuation of the laser energy leads to significant error in phase measurement.

For isolated attosecond pulse generation, the laser intensity in the gas target must be kept below the ionization saturation intensity, which is $< 10^{15}$ W/cm² for argon. Therefore, the high-power laser beam is loosely focused with a 6.5-m-focal length mirror. Figure 4 shows the focal spot profile with a line-out in both the vertical and horizontal direction. The diameter of the focal spot is 0.31 mm (FWHM). The corresponding long confocal length allows the usage of a long gas cell with low gas density, which showed high conversion efficiency in producing coherent femtosecond XUV pulses with HHG.¹⁰

The laser field for GDOG is obtained by transforming the 15 fs linearly polarized field with a set of birefringent optics.⁴ To achieve a gate width less than one optical cycle, the laser pulses are sent through a 1.070 mm quartz plate,

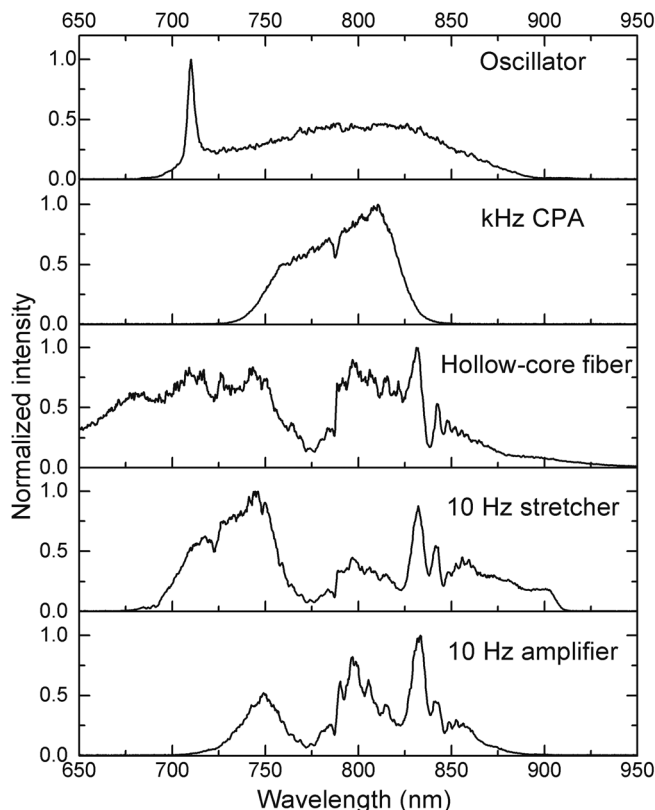


FIG. 2. Spectra taken at successive stages of the laser system.

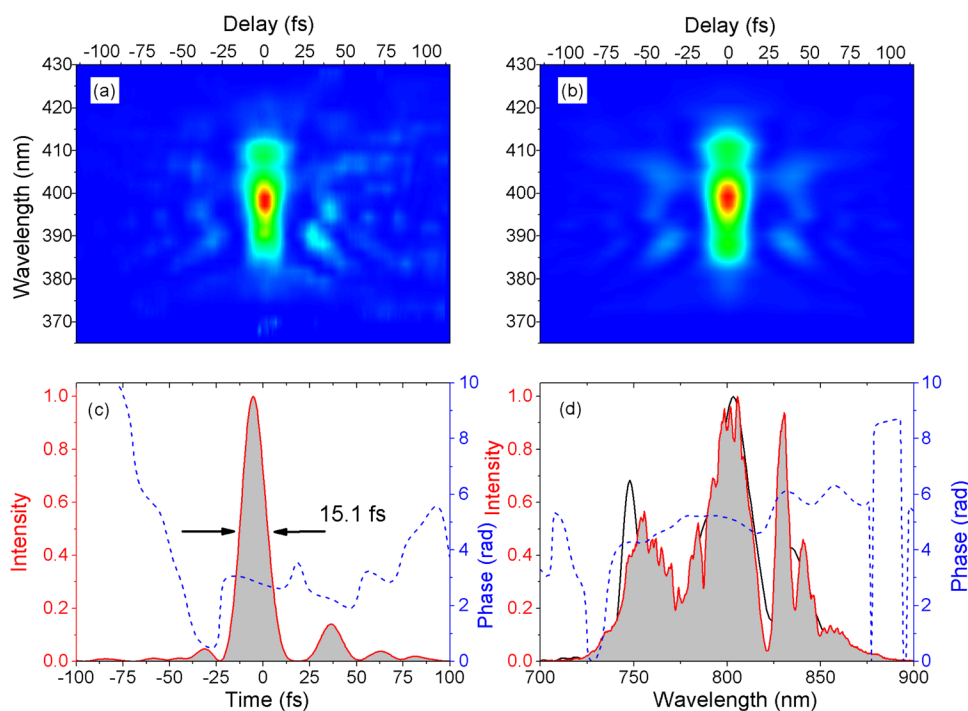


FIG. 3. Characterization of the 15.1 fs laser pulse by SHG FROG. (a) The measured FROG trace. (b) The reconstructed FROG trace. (c) The retrieved pulse shape (solid line) and phase (dashed line). (d) The retrieved power spectrum (solid back line) and phase (dashed line) with the independently measured spectrum (solid red line).

three 0.3 mm BK7 Brewster windows, a 0.440 mm quartz plate, and a 0.141 mm barium borate crystal (BBO) located directly after the focusing mirror. After the GDOG optics, the focused laser beam enters a 100 mm-long gas cell, where attosecond pulses were generated in argon held at 4 Torr. Both ends of the cell were sealed with glass windows, each having 1 mm-diameter holes through which the NIR beam and XUV beam can pass. To eliminate the residual driving laser that propagates collinearly with the XUV light, the output beam from the gas cell was filtered by two silicon mirrors set at the Brewster angle of the NIR laser.¹¹

The XUV spectra under various gating conditions were measured with a home-built high-resolution XUV grating spectrometer.¹² Figure 5 shows single-shot HHG spectra of argon while using no gating (800 nm linearly polarized pulse), two-color gating (a second-harmonic field added to the linear fundamental field), and GDOG. As expected, well-resolved odd harmonics were generated when no gating was applied, and both odd and even harmonics appeared with the two-color laser field. These peaks merged to a continuum for

every laser shot under the GDOG field. The profile of the XUV spectrum generated with GDOG changed from shot to shot, and we are working on determining the correlation between the spectrum shape and the CEP by tagging the phase value with the single shot XUV spectrum. If the dispersion of the XUV spectrum were to be compensated to the Fourier-transform limit by an appropriate method,¹³ the corresponding pulse duration would be 230 as.

The energy of the XUV pulse was measured to be 0.5 nJ with an XUV photodiode (Opto Diode Corp.) placed behind two 300 nm-thick aluminum filters. This corresponds to an estimated XUV energy generated at the exit of the gas cell of 100 nJ, assuming a 50% reflectance off each of the two silicon mirrors and a 2% total transmission through the two filters with 20 nm oxidation layers.

In conclusion, we have developed a 15 fs, 13 TW high-power laser system with a 10 Hz repetition rate for generating high-flux isolated attosecond pulses. This system represents the highest extent to which white-light from a hollow-core fiber has been amplified, allowing the pulses to

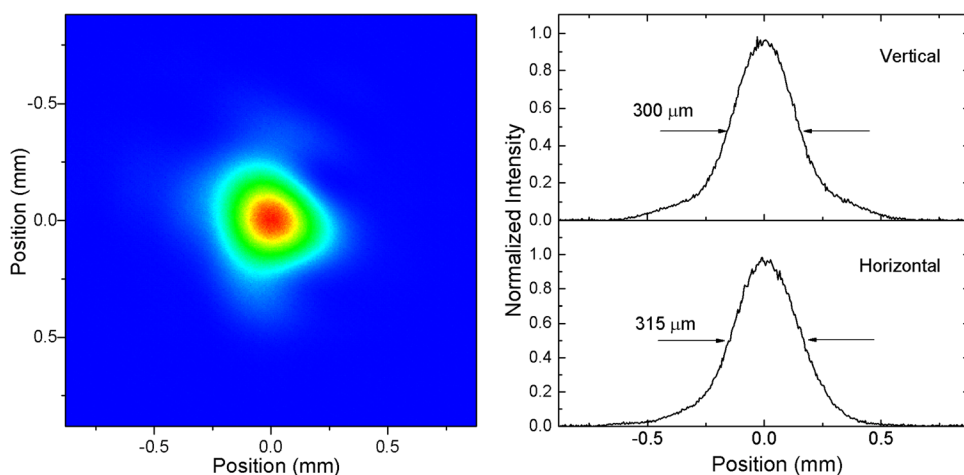


FIG. 4. Left: Intensity profile measurement at focus of $f = 6.5$ m mirror with a 12-bit CCD camera; right: horizontal and vertical line-out (diameter is 310 μm at half-maximum).

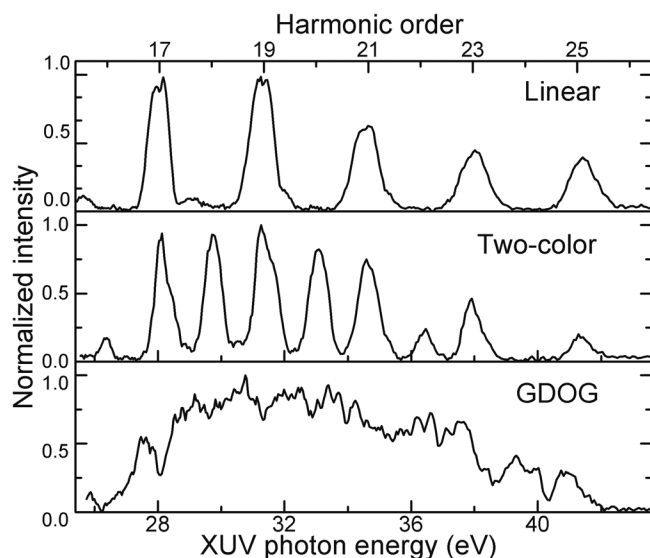


FIG. 5. Single-shot XUV spectra generated in argon under different gating conditions.

achieve high energy without incurring substantial gain narrowing. This is also the first demonstration of using multi-cycle laser pulses at the 10 TW level with the GDOG technique to generate an XUV continuum. Our preliminary

results pave the way for scaling up XUV photon flux by further increasing the power of the driving laser.

This material is based upon work supported by the U.S. Army Research Office and the National Science Foundation under Grant Number 1068604. Huaping Zang and Xiaowei Wang recognize the support from the China Scholarship Council.

¹F. Krausz and M. Ivanov, *Rev. Mod. Phys.* **81**, 163 (2009).

²Z. Chang and P. Corkum, *J. Opt. Soc. Am. B* **27**, 9 (2010).

³F. Ferrari, F. Calegari, M. Lucchini, C. Vozzi, S. Stagira, G. Sansone, and M. Nisoli, *Nature Photon.* **4**, 875 (2010).

⁴X. Feng, S. Gilbertson, H. Mashiko, H. Wang, S. D. Khan, M. Chini, Y. Wu, K. Zhao, and Z. Chang, *Phys. Rev. Lett.* **103**, 183901 (2009).

⁵J. Seres, A. Müller, E. Seres, K. O'Keeffe, M. Lenner, R. Herzog, D. Kaplan, C. Spielmann, and F. Krausz, *Opt. Lett.* **28**, 1832 (2003).

⁶H. Takada and K. Torizuka, *IEEE J. Quantum Electron.* **12**, 201 (2006).

⁷A. Amani Eilanlou, Y. Nabekawa, K. L. Ishikawa, H. Takahashi, and K. Midorikawa, *Opt. Express* **16**, 13431 (2008).

⁸K. Ertel, C. Hooker, S. J. Hawkes, B. T. Parry, and J. L. Collier, *Opt. Express* **16**, 8039 (2008).

⁹K.-H. Hong and C. H. Nam, *Jpn. J. Appl. Phys. Part 1* **43**, 5289 (2004).

¹⁰E. Takahashi, Y. Nabekawa, T. Otsuka, M. Obara, and K. Midorikawa, *Phys. Rev. A* **66**, 021802 (2002).

¹¹E. J. Takahashi, Y. Nabekawa, H. Mashiko, H. Hasegawa, A. Suda, and K. Midorikawa, *IEEE J. Quantum Electron.* **10**, 1315 (2004).

¹²X. Wang, M. Chini, Y. Cheng, Y. Wu, and Z. Chang, *Appl. Opt.* **52**, 323 (2013).

¹³K. Zhao, Q. Zhang, M. Chini, Y. Wu, X. Wang, and Z. Chang, *Opt. Lett.* **37**, 3891 (2012).